

Direct Determination of Lead in Airborne Particulate Matter
by Graphite Furnace Atomic Absorption Spectrometry

By

LAI Yuen Kwan

A Thesis Submitted to the Environmental Science Programme

Graduate School, The Chinese University of Hong Kong

in Partial Fulfillment of The Requirement

for the degree of

Master of Philosophy

(June, 1997)

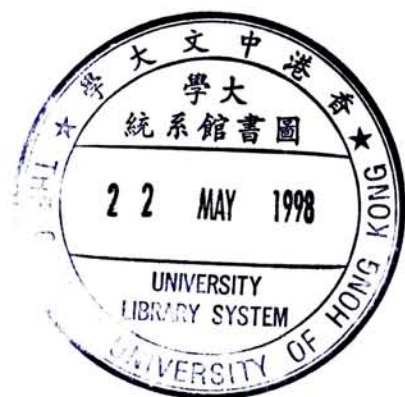
Thesis Committee:

Prof. Kevin W. P. Leung (Chairperson)

Prof. P. K. Hon

Prof. Jimmy C. M. Yu

Prof. Frank S. C. Lee (External Examiner)



Abstract

A new method for the determination of metal contents in air particulates by graphite furnace atomic absorption spectrometer (GFAAS) has been developed. Air particulates collected on a Teflon filter were suspended in a viscous organic solvent with ultrasonic agitation. The suspension behaviors of the air particulates in two organic solvents, 1-decanol and ethylene glycol, were studied by monitoring the change in mean particle size of particulate matter with time by Laser Light Scattering (LLS). Ethylene glycol was better than 1-decanol on stabilizing the particulate matter in a fluid media. Hence, ethylene glycol was chosen in the subsequent studies. The slurry suspension resulted was introduced directly into a graphite tube for atomization and the metal contents in the sample was determined by standard addition method.

The recovery study of Lead in NIST Standard Reference Material - Urban Particulate Matter (SRM 1648), using developed method with non-linear standard addition, was between 91 - 107 %. The amount of Lead in air particulates of Cape D'Aguilar, Hong Kong analyzed by developed method and acid digestion method was $27 \pm 3 \text{ ng/m}^3$ and $22 \pm 3 \text{ ng/m}^3$ respectively. The two methods showed a good agreement between each other. The detection limit and precision of developed method was found to be 10 ng/m^3 for Pb and $\pm 10 \%$ respectively. This method offers a quick and efficient alternative for air pollution studies.

Acknowledgement

I would like to express my sincere thanks to my supervisor Prof. Jimmy C. M. Yu for his guidance and advice on my research work and the preparation of this thesis.

Thanks are also given to the graduate students Miss Chan Yuk-Lin, Miss Cheng Lai-Nor and Mr. Lin Jun in our laboratory for their helpful assistance and discussions.

I am also indebted to Prof. S. C. Lee at the Civil and Structural Engineering Department of the Hong Kong Polytechnic University for providing air particulate samples.

June, 1997

LAI Yuen Kwan

Environmental Science Programme

The Chinese University of Hong Kong

Contents

	Page
Abstract.....	i
Acknowledgement.....	ii
Contents.....	iii
List of Figures.....	vi
List of Tables.....	vii
1. INTRODUCTION	
1.1 Air Pollution in Hong Kong.....	1
1.2 Lead in Air and its Harmful Effects on Human.....	3
1.3 Sampling of Air Particulates.....	6
1.3.1 Principles of filter sampling.....	6
1.3.2 Filter media for air sampling.....	7
1.4 Sample Treatment.....	9
1.4.1 Acid digestion - standard method for analysis of metals.	9
1.4.2 Slurry sampling - direct method for analysis of metals...	9
1.4.3 Literature survey on slurry sampling.....	10
1.4.4 Comparison between acid digestion and slurry sampling methods.....	10
1.5 Instrumental Analysis.....	11
1.5.1 Graphite furnace atomic absorption spectrometry.....	11
1.5.2 Background correction by the Zeeman effect.....	12
2. EXPERIMENTAL	
2.1 Apparatus.....	14

2.2	Reagents.....	14
2.3	Procedure.....	15
2.3.1	Selection of sample introduction technique.....	15
2.3.2	Recovery study of lead in standard reference material (SRM) in 1-decanol.....	16
2.3.3	Study of suspension behavior of solvents with SRM.....	16
2.3.4	Recovery study of lead in SRM in ethylene glycol.....	17
2.3.5	Determination of lead in SRM by the developed method	17
2.3.6	Determination of lead in SRM by the acid digestion method.....	18
2.3.7	Application of the developed method on the analysis of real sample.....	18
3.	RESULTS AND DISCUSSION	
3.1	Choice of Solvents for Suspension of Air Particulates.....	20
3.2	Sample Introduction Technique.....	20
3.3	Recovery Study of lead in SRM in 1-Decanol.....	22
3.3.1	Drying stage of the temperature program for analysis....	23
3.3.2	Effect of 1-decanol on the absorbance signal of the analyte.....	24
3.3.3	Sample injection volume.....	25
3.3.4	Design of temperature program for analysis.....	25
3.4	Study of Suspension Behavior of Solvents.....	27
3.5	Recovery Study of lead in SRM in Ethylene Glycol.....	32

3.6	Evaluation of the Developed Method.....	33
3.6.1	Determination of lead in SRM.....	33
3.6.2	Application of non-linear standard addition method.....	35
3.6.3	precision and accuracy of the developed method.....	36
3.7	Recovery Study with the Acid Digestion Method.....	36
3.8	Analysis of Real Sample by the Developed Method.....	37
3.8.1	Principles of TEOM [®] on mass measurement.....	37
3.8.2	Selection of filter media for air sampling.....	37
3.8.3	Study of dislodging efficiency of air particulates from Teflon filter.....	38
3.8.4	Comparison with the acid digestion method.....	39
4.	CONCLUSION.....	40
5.	REFERENCES.....	41
6.	APPENDIX.....	46

List of Figures

<u>Number</u>	<u>Description</u>	<u>Page</u>
1	Annual average concentrations of lead derived from RSP during 1989 - 1994.	4
2	Distribution of lead derived from RSP of Hong Kong in 1994.	5
3	Variation of absorbance against lead concentration with (a) Direct Introduction and (b) Platform in Tube technique.	21
4	Distribution of the particle size of Urban Particulate Matter in ethylene glycol.	30
5	Distribution of the particle size of Urban Particulate Matter in 1-decanol.	31
A1	Schematic diagram of sampling device.	49
A2	Graphite tube with platform inside (A) exposed view (B) end view.	50

List of Tables

<u>Number</u>	<u>Description</u>	<u>Page</u>
1	Comparison between acid digestion and slurry sampling method.	10
2	Temperature program employed for the analysis of Lead in GFAAS.	16
3	Comparison between ethylene glycol and 1-decanol based on their properties.	20
4	Amount of lead in SRM under (a) 1-decanol (b) acid digestion.	23
5	The change in recovery with the volume of 1-decanol added.	24
6	Parameters employed for the analysis of lead by GFAAS.	26
7	Amount of lead in SRM under 1-decanol (by new analytical parameters).	26
8	Comparison of the suspension behavior of ethylene glycol and 1-decanol.	28
9	Amount of lead in SRM under ethylene glycol.	32
10	The absorbance data of Pb in sample by GFAAS.	33
11	Comparison between measured and certified concentration of Pb in SRM.	33
12	Curve fitting results using non-linear regression program.	35
13	Comparison between measured and certified concentration of Pb in SRM with non-linear standard addition based on ethylene glycol.	36

14	The absorbance data of lead in real sample.	39
15	Curve fitting results using non-linear regression model (real sample).	39
16	Comparison between the developed and acid digestion method on the analysis of lead in real sample.	39
A1	Certified values of constituent elements in SRM 1648.	51

1. Introduction

1.1 Air Pollution in Hong Kong

People in Hong Kong have been increasingly aware of the air pollution problems. Checking the Air Pollution Index (API)¹ before going out becomes a common practice of the residents. API is a means for the concise representation of information on air quality. It provides a simple and uniform way to report daily air pollution concentrations and serves as a basis for issuing advice to the public before the onset of air quality episodes. This will enable everyone, particularly susceptible groups, such as people with heart or respiratory illness, to consider taking precautionary measures when necessary. The government has put a lot of effort into monitoring the air quality in Hong Kong, but it still has room for improvement.

The main sources of air pollution are manufacturing industries, power generation, construction work, and road traffic.² Although power stations emit the largest quantity of air pollutants, their location and pollution control specifications ensure that not many people are affected. The main urban air polluters are industries and road traffic. Dust pollution from construction activity is also a major concern, given its proximity to populated areas. Industrial sources include chimneys of the factories that produce dark smoke and non-stop emission of dust and grit. Air pollution from this source has become less serious in recent years. It is due to the use of cleaner industrial fuels, licensing controls of specified industrial processes and the restructuring of Hong Kong's manufacturing industry.

Pollution from motor vehicles continues to be a problem, despite the wider use of less-polluting fuels (unleaded petrol, low-sulphur diesel) and stricter emission

requirement for newly registered vehicles. It was due to the predominance of diesel engine and the continued growth in vehicle numbers. The government had introduced stringent emission standards for new petrol-engined vehicles, requiring catalytic converters to be fitted, and for light duty diesel-engined vehicles. Rapid improvements in air quality can best be achieved by requiring all smaller vehicles (including all taxis and public light buses) to operate on unleaded petrol. Public consultation took place in late 1995 on proposals to phase out, over five years, the use of diesel fuel for all vehicles below four tonnes in weight, in order to eliminate a major emission source of respirable suspended particulates.

Environmental Protection Department (EPD) had set up air quality monitoring stations throughout Hong Kong to determine the air quality in the territory. Pollutants such as sulphur dioxide, nitrogen dioxide, carbon monoxide, ozone, total suspended particulates (TSP) and respirable suspended particulates (RSP) were monitored in these stations. TSP are airborne particles of different sizes ranging from approximately 0.1 to 100 μm . These airborne particles include smoke, fumes, dust and fly ash of various sizes, shape and composition. RSP are the fraction of the total suspended particulates which have a particle size of 10 μm or less, in diameter. These smaller particles are most likely to be inhaled and deposited into the thoracic region of the lung. It has harmful effects on the pulmonary function such as reduced lung function, respiratory illness and even posing a cancer risk for certain particles. Among the various pollutants monitored, RSP still constitutes a problem as the annual RSP levels were generally high throughout the territory as 5 out of 8 monitoring stations exceeded the annual Air Quality Objectives (AQO) in 1994.³

1.2 Lead in Air and its Harmful Effects on Human

Lead is one of the chemical constituents that is found in the RSP in Hong Kong. It mainly comes from the combustion of leaded petrol. Figure 1 shows the annual average concentration of lead derived from RSP during 1989 - 1994.⁴⁻⁹ It indicated that there was an increasing trend of lead level in Hong Kong, from 58 ng/m³ in 1989 to 72.5 ng/m³ in 1994. It may be due to the increase of vehicle emissions during these years.

The distribution of lead level in RSP of Hong Kong during 1994 is shown in Figure 2.⁹ The high levels of lead were found in regions of heavy traffic such as Tai Po, Mong Kok and Tsuen Wan. The largest source of lead in the atmosphere has been from leaded petrol combustion in motor vehicles, but with the introduction of unleaded petrol, air lead levels have decreased considerably. Other airborne sources include combustion of solid waste, coal, and oils, emissions from iron and steel production and lead smelters, and tobacco smoke. Exposure to lead can also occur from food and soil.

Acute exposure to high levels of lead in humans causes brain damage, kidney damage and gastrointestinal distress.¹⁰ Chronic exposure to lead in humans results in effects on the blood, central nervous system (CNS), blood pressure, kidneys, and Vitamin D metabolism. Children are particularly sensitive to the chronic effects of lead, with slowed cognitive development, reduced growth and other effects reported. Reproductive effects, such as decreased sperm count in men and spontaneous abortions in women, have been associated with lead exposure. The developing fetus is at particular risk from maternal lead exposure, with low birth weight and slowed postnatal neurobehavioral development noted. In view of the adverse effects on humans, the lead content in RSP of air should be closely monitored.

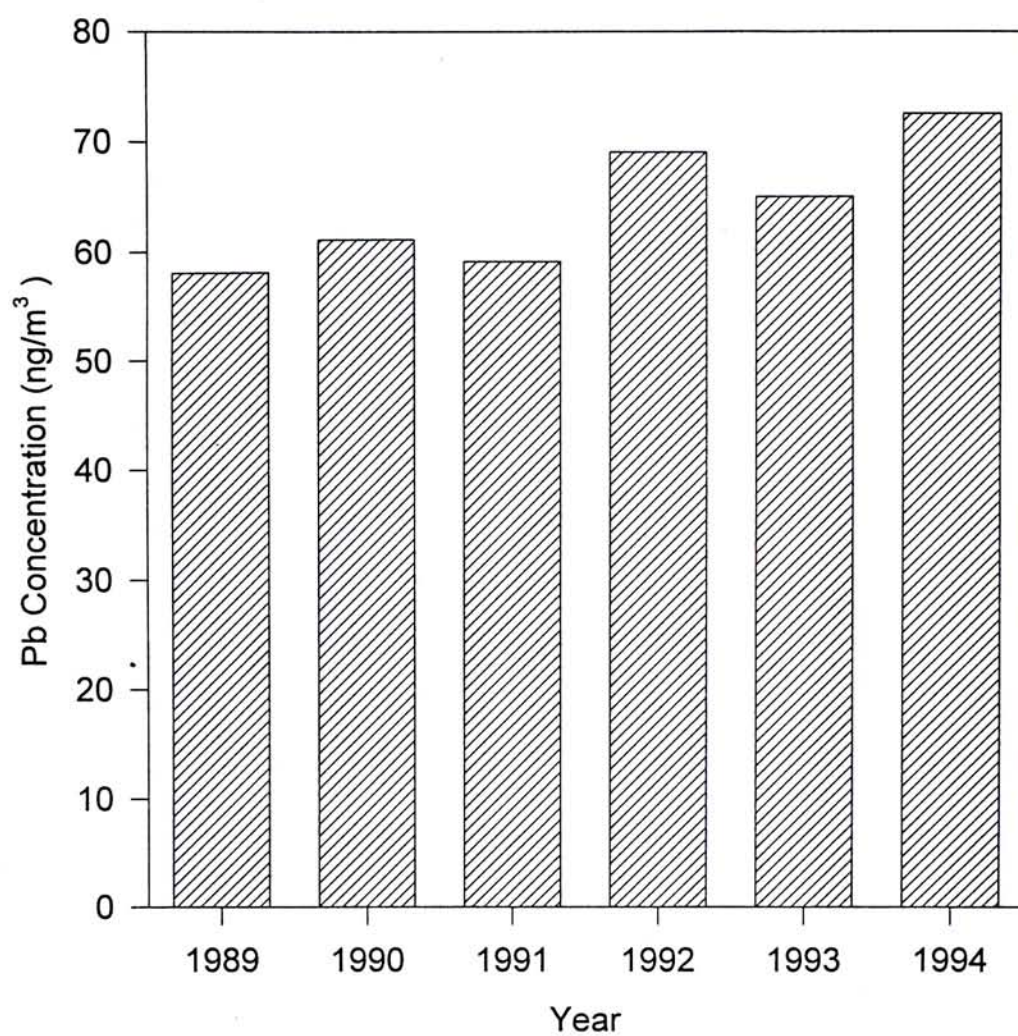


Figure 1. Annual average concentrations of lead derived from RSP during 1989 -1994.

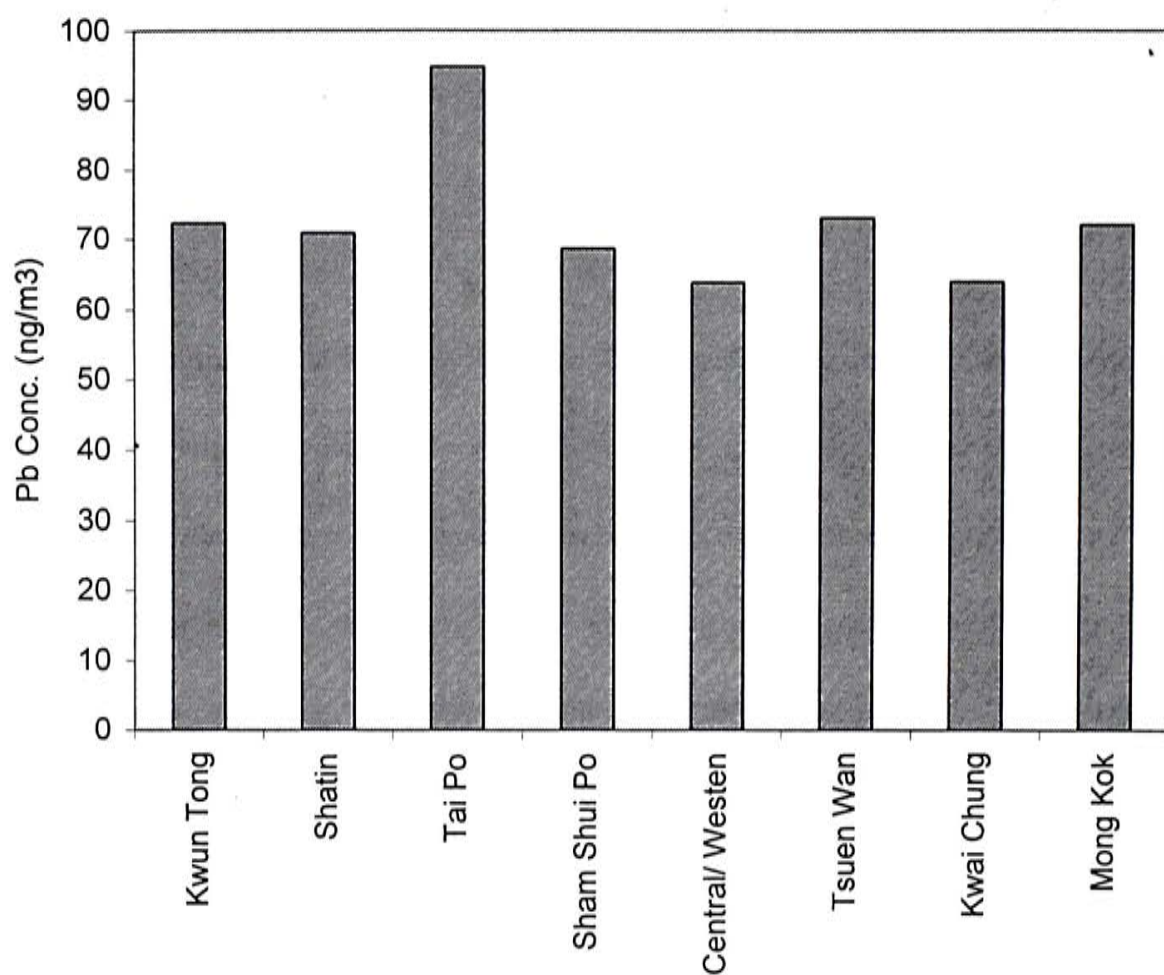


Figure 2. Distribution of lead derived from RSP of Hong Kong in 1994.

1.3 Sampling of Air Particulates

1.3.1 Principles of filter sampling

The essential components of a filter sampling system for aerosol measurement include a sampling probe, a filter holder, a flow measurement device, a flow regulator and a pump. Aerosol-laden air is drawn through a sampling probe for isokinetic sampling from a flow stream into a filter holder containing an appropriately selected filter medium. The aerosol is separated from the flow stream to the extent dictated by the characteristics of the filter, the air velocity through the filter, and other factors such as the particulate loading on the filter. The air drawn through the filter flows to a flow measurement device such as a rotameter, mass flow meter, or dry test meter, and then into a flow regulating mechanism, such as an orifice or valve coupled with an air moving device or pump. Selecting the appropriate components and the optimum order for the flow progression through the system is crucial in achieving a representative sample of the aerosol on the filter.¹¹

The effectiveness with which the sampling probe extracts the aerosol from a moving air stream is termed the “aspiration efficiency” of the inlet. In addition to the limitations imposed by aerosol dynamical behavior on inlet aspiration efficiency, particle losses due to temperature gradients between the probe inlet surfaces and the air stream, and electrostatic deposition losses due to charged probe inlet surfaces, particularly in the case of those made with plastic materials, must also be considered.

In many instances, the geometry of the sampling environment necessitates a length of connecting tubing between the inlet probe and the filter holder. The passage of the aerosol from the inlet to the filter holder is characterized by the “transport efficiency” and is influenced by a number of factors such as gravitational,

diffusional, and inertial deposition onto the wall surfaces, as well as temperature-gradient-related and electrostatic wall loss effects.¹² It is critical that the aspiration and transport efficiencies of a filter sampling system be determined in each application to adequately characterize any distortion in the aerosol size distribution or concentration obtained on the sampling filter. Maximizing these efficiencies is particularly critical due to their inherent particle size dependence, making corrections for sampling biases extremely difficult if the aerosol size distribution is unknown. In general, sampling losses are minimized by locating the filter holder as close as possible to the sampling inlet probe, and if possible, sampling with no inlet probe or connecting tubing upstream of the filter.

1.3.2 Filter media for air sampling

Filtration is a common method for aerosol measurement. It is done by collection, through removal from the gas phase, of a representative sample of the aerosol on a suitable porous medium or filter. In general, filter media can be divided into 4 types according to their characteristic structure:¹³

1. Fibrous filters

Fibrous filters consist of a mat of individual fibers. The materials used for making it include cellulose, glass, quartz and plastic fibers. They are used widely for general-purpose air sampling.

2. Porous membrane filters

Porous membrane filters have a very complicated and uniform microstructure providing a tortuous or irregular air flow path. A variety of filters made of cellulose esters, polyvinyl chloride and Teflon are available. Its applications include monitoring metals, dust and asbestos in air.

3. *Straight-through pore filters*

Straight-through pore filters are thin polycarbonate films with cylindrical pores perpendicular to film surface. They are widely used for particle analysis using surface analytical techniques such as light and electron microscopy.

4. *Granular-bed filters*

Granular-bed filter performs aerosol measurement by passing particle-laden air through a bed consisting of granules and recovering aerosols afterwards by extraction procedures. The granules commonly used are activated charcoal, glass and quartz.

1.4 Sample Treatment

1.4.1 Acid digestion - standard method for analysis of metals

Acid digestion is one of the oldest and still most frequently used technique in decomposing samples for subsequent analysis. Mineral acids and mostly oxidizing acids such as concentrated nitric acid are the common reagents for this purpose. Most inorganic materials will dissolve in acids or mixtures of acids, although some volatile elements may be lost in the process.¹⁴

Acid digestion has the advantage of being effective on both inorganic and organic materials. It often destroys or removes the sample matrix, thus helping to reduce or eliminate some type of interference. Acid digestion may give rise to systematic errors due to contamination caused by reagents and container material, losses of elements caused by adsorption on the surface of the vessel and losses of elements by volatilization.¹⁴

1.4.2 Slurry sampling - direct method for analysis of metals

Direct solid sampling is a technique in which the sample is introduced directly into analytical instrument for analysis without tedious digestion step. However, sample introduction and calibration will be a problem. The introduction of a suspension of the finely powdered sample (slurry) combines both the advantages of liquid and solid sampling. It permits sample introduction using micropipettes and autosamplers and the sample in slurried form will be much more homogeneous. Sample can be easily calibrated with standards by slurry technique.¹⁵

Slurry sampling lowers the detection limit and avoids sample dissolution. The technique is applicable to the analysis of inorganic and organic materials in the form of powders, sheets, samples of soft and hard tissues, etc.

1.4.3 Literature survey on slurry sampling

Slurry sampling has wide applications in environmental analysis. The sample of interest ranges from sediments to biological substances. One of the applications of slurry sampling is the determination of the metal contents in air particulates by atomic absorption spectrometry.¹⁶⁻¹⁷

Slurry preparation in aqueous solution is rarely suitable because of the rapid sedimentation of the powdered samples. The slurry can be stabilized using a highly viscous medium. Most slurried food and plant samples employ Triton X-100 as a suspending reagent for analysis.¹⁸⁻²⁴ Other applications of interest include sediment and soil,²⁵⁻³² cereal and dairy products,³³⁻⁴⁰ seafood⁴¹⁻⁴² and body fluid.⁴³⁻⁴⁴

1.4.4 Comparison between acid digestion and slurry sampling methods

The characteristics of these two methods are summarized in Table 1.

Table 1. Comparison between acid digestion and slurry sampling method.

<i>Acid Digestion Method</i>	<i>Slurry Sampling Method</i>
<ul style="list-style-type: none">• Heating is required• More prone to contamination• Long treatment time (hours)• Aqueous samples result	<ul style="list-style-type: none">• No heating is required• Less prone to contamination• Short treatment time (minutes)• Non-aqueous samples usually result

1.5 Instrumental Analysis

1.5.1 Graphite furnace atomic absorption spectrometry^{14, 45}

Graphite furnace or electrothermal atomic absorption spectrometry (GFAAS) was first developed in the 1960's. GFAAS generally provides enhanced sensitivity as compared with flame AAS, because the entire sample is atomized in a short period and the average residence time of the atoms in the optical path is a second or more. Electrothermal atomizers are used for atomic absorption and atomic fluorescence measurements but have not been generally applied for emission work. They are, however, beginning to be used for vaporizing samples in inductively coupled plasma emission spectroscopy.

Electrothermal atomizers are small electrically heated tubular furnaces. The furnace is a graphite tube 3 - 5 cm long and 3 - 8 mm in diameter. The tube is coated with pyrolytic graphite to lower the loss of atomic vapor by diffusion through the tube wall, improve residence time and increase the resistance to chemical attack.

The furnace is positioned so that the radiation from the line source is directed through the tube. A hole in the top of the tube allows 5 - 100 μ l of solution to be injected manually with a micropipette or with an automatic injector. Each end of the furnace tube is connected to a high current, programmable power supply through water-cooled contacts. The power supply controlling the furnace can be programmed to dry, ash and atomize the sample at the appropriate temperatures.

An inert internal gas stream such as argon enters the two ends of the tube and leaves the tube via the central sample tube. This stream not only excludes air but also carries away vapors generated from the matrix during the drying and ashing

steps. In the atomization step, the internal gas flow is generally stopped in order to prevent cooling and removal of the atom vapor during atomization.

Electrothermal atomizers offer the advantage of unusually high sensitivity for small volumes of sample. Typically, sample volumes between 0.5 - 10 μL are employed; under these circumstances, absolute detection limits typically lie in the range of 10^{-10} to 10^{-13} g of the analyte. The relative precision of GFAAS is generally in the range of 5 to 10 %. However, furnace methods are slow - typically requiring several minutes per element. Another disadvantage is that the linear range is limited, being usually less than two orders of magnitude.

1.5.2 Background correction by the Zeeman effect

The atomic spectrum, both the emission and absorption lines, placed in a magnetic field of approximate 1 tesla is split into several components and is subjected to polarization. This is known as Zeeman effect.

Zeeman background correction in atomic absorption spectrophotometer (AAS) is based on the splitting of atomic spectral lines into several components under the influence of a magnetic field. Either the line source (direct Zeeman AAS) or the atomizer (inverse Zeeman AAS) is placed between the poles of a strong magnet.

The Hitachi Z-8200 Graphite Furnace AAS is a model that employs inverse Zeeman effect. By this technique, the permanent magnet is placed around the atomizer. The absorption line of the analyte atoms is split into π - and σ -components. The magnetic field is perpendicular to the optical axis and a polarizer is used to separate the radiation beam from the hollow cathode lamp into 2 components.

One of the components oscillates parallel to the magnetic field and the other perpendicular to it. Both components have the same wavelength. When the parallel component is transmitted, it will be absorbed by the central unshifted π -component of the analyte (the sample element and background both absorb the light). In the next quarter cycle only the perpendicular source light is transmitted. This perpendicular light will not be absorbed by the central π -component of the analyte (although it is at exactly the same wavelength) because its polarization is different. Therefore, only background absorbs in this case. Subtraction of the signal of the perpendicular polarized component from that of the parallel component corrects for background absorption.

2. Experimental

2.1 Apparatus

All samples were analyzed by a Hitachi Z-8200 polarized Zeeman graphite furnace atomic absorption spectrophotometer. A porous electrographite platform was placed inside the pyrolytically coated graphite tube to improve the atomization process. The platform had the dimension of 8 mm long, 3 mm wide and 0.5 mm thick. The graphite tube with the platform in it was cleaned at temperature above 2500 °C for 10 seconds in the GFAAS prior to use. A Coulter LS-230 enhanced laser diffraction particle size analyzer with micro volume module installed was used to determine the particle size of air particulates and its suspension behavior in different solvents. Air particulate samples were collected on 47 mm Teflon filters by Rupprecht & Patashnick TEOM[®] Series 1400a ambient particulate monitor. A Branson 3210 ultrasonic bath with timer was employed to dislodge the air particulates from the filter media.

2.2 Reagents

Lead standard solutions with different concentrations were prepared from diluting a 1000 ppm lead standard (High Purity Standards) with ultra-pure water. Analytical reagent grade nitric acid (65 %), 1-decanol and ethylene glycol were purchased from RDH and used as received. Standard reference material (Urban Particulate Matter), SRM 1648, was purchased from National Institute of Standards and Technology (NIST) and used as received.

2.3 Procedure

2.3.1 Selection of sample introduction technique

Lead stock standards (10 - 50 ppb) were introduced into the GFAAS with the following technique:

1. Direct introduction

The graphite tube was decontaminated by firing at high temperature in graphite furnace. Then 20 μL of metal stock solution was injected into the graphite tube by micropipet and the sample was analyzed by GFAAS. The procedure was repeated with different stock concentrations until a calibration curve was obtained.

Table 2 gives the temperature program employed.

2. Lead \rightarrow platform in tube

The graphite platform ($3 \times 8 \times 0.5$ mm) was inserted into the graphite tube with a stainless steel fine forceps (Figure A2). The graphite tube with platform inside was decontaminated by firing at high temperature in the graphite furnace. A 20 μL of metal stock solution was injected on the platform by micropipet. The graphite tube with platform was then put into the GFAAS for analysis. The procedure was repeated with different stock concentrations to obtain a calibration curve. The linearities of the calibration curves based on these two sample introduction techniques were compared.

Table 2. Temperature program employed for the analysis of lead in GFAAS.

<i>Stage</i>	<i>Start (°C)</i>	<i>End (°C)</i>	<i>Ramp (s)</i>	<i>Hold (s)</i>
Drying	80	140	40	
Ashing	400	400	30	
Atomizing	2000	2000		10
Cleaning	2200	2200		4
Cooling				5

2.3.2 Recovery study of lead in Standard Reference Material (SRM) in 1-Decanol

Approximately 10 mg of SRM was weighed and suspended in 100 mL 1-decanol. In order to make a stable suspension, ultrasonic agitation of samples for 30 minutes was employed. It was then diluted to a suitable concentration for subsequent analysis.

A 20 μ L diluted slurried sample was pipetted out manually and injected into a graphite tube of GFAAS for analysis.

The temperature program was the same as before except the upper limit of the drying step was increased to 200 °C.

The factors such as the design of temperature program and sample injection volume were studied. A table showing the certified values of constituent elements in SRM 1648 is shown in Table A1.

2.3.3 Study of suspension behavior of solvents with SRM

Electrical offset measurement, laser beam alignment and background measurement were performed by laser light particle size analyzer. SRM was then

added to the selected solvent in the micro volume module of the analyzer until about 10 % obscuration was reached. The sample was thoroughly mixed by the magnetic stirrer inside the module. Then the mean particle size of particulate matter in the solvent was measured. After taking the measurement, the stirrer was turned off. The measurement was taken again after 5 minutes. The suspension behavior of the solvent was evaluated based on the change in mean particle size of particulate matter with time. The procedure was repeated with another selected solvent to evaluate its suspension behavior of SRM.

No calibration was required for this analyzer as the calibration was determined by the optical design. All necessary adjustments were made by measuring electrical offsets and aligning the laser beam.

2.3.4 Recovery study of lead in SRM in Ethylene Glycol

Approximately 10 mg of SRM was weighed and suspended in 100 ml ethylene glycol. In order to make a stable suspension, ultrasonic agitation of samples for 30 minutes was employed. It was then diluted to a suitable concentration for subsequent GFAAS analysis.

A 10 μ L diluted slurried sample was pipetted out manually and injected into a graphite tube of GFAAS for analysis. The temperature program employed was the same as before except the upper limit of drying step was increased to 280 °C and the duration of drying step was increased to 100 s.

2.3.5 Determination of lead in SRM by the developed method

Approximately 20 mg of SRM was weighed out and suspended in 100 ml ethylene glycol. A 25 mL slurried sample was diluted to 100 ml with ethylene glycol

for subsequent analysis. A 10 μL diluted slurried sample was pipetted out and analyzed in GFAAS. After the analysis, a 20 μL lead standard (500 ppm) was injected into the 100 mL slurried sample and mixed thoroughly. The content of lead in sample was determined in GFAAS.

The procedure was repeated with 3 more additions to construct a calibration curve. The actual concentration of lead in original sample was determined by standard addition method.

2.3.6 Determination of lead in SRM by the acid digestion method

Approximately 10.6 mg SRM was weighed out and dissolved to 50 ml nitric acid (65 %). The sample was digested for 2 hours on a hot plate. After the digestion, it was diluted with ultra-pure water. The content of lead in sample was determined by GFAAS.

2.3.7 Application of the developed method on the analysis of real sample

Air particulate samples with aerodynamic diameter less than 10 μm (respirable suspended particulates, RSP) was collected on Teflon filter (47 mm diameter and 0.8 μm pore size) at Cape D'Aguilar, Hong Kong in November, 1996. The flow rate was maintained at 14 L/min and the sampling time was 24 hours.

The mass of Teflon filter loaded with air particulates was weighed by an electronic balance. Then 10 mL ethylene glycol was added to the filter in a beaker. It was put in ultrasonic bath for 30 minutes so as to facilitate the dislodging of air particulates from the Teflon filter to ethylene glycol. After ultrasonic agitation, the Teflon filter was removed and dried in an oven at about 100 $^{\circ}\text{C}$ for 2 hours to remove the remaining solvent on filter surface. The mass of Teflon filter after drying was

determined. Ethylene glycol with air particulates suspended was divided into two equal portions for subsequent analysis.

The actual content of lead in sample was determined by standard addition method. A 10 μ L slurried sample was pipetted out and injected into the GFAAS for analysis. Then 20 μ L lead standard (25 ppm) was added to the 5 mL slurried sample and mixed thoroughly. 10 μ L slurried sample was again injected into GFAAS for analysis. The procedure was repeated until 4 data points were obtained for the construction of calibration curve.

A portion of the slurried sample was treated by acid digestion. A 5 mL slurried sample in a beaker was dried on a hot plate. After drying, acid digestion of the air particulates was carried out with 2 mL concentrated nitric acid (65 %). Then the digested sample was diluted with ultra-pure water and the content of lead in sample was determined by GFAAS.

3. Results and Discussion

3.1 Choice of Solvents for Suspension of Air Particulates

In slurry sampling, the role of the solvent is to provide a stable and uniform suspension for analysis. Several requirements should be met in choosing a suitable solvent for suspending the air particulates: (1) It should be of high viscosity so that it can suspend the particulate matter well and hence provide a uniform distribution of it in the solvent media. (2) It should have low toxicity so as to dispose it safely and will not produce additional pollutants to the environment. (3) It should vaporize at moderate temperature, such as during the drying step of the temperature program of GFAAS. (4) It should be inert so as not to interact with the particulate matter inside. In view of these requirements, two solvents were chosen and some of their properties are given in Table 3.

Table 3. Comparison between ethylene glycol and 1-decanol based on their properties.

<i>Properties</i>	<i>Ethylene Glycol</i>	<i>1-Decanol</i>
Viscosity (mPa-s) ^{(a), (b)}	16.1	10.9
Toxicity	Low	Low
Boiling Point (°C)	197	232
Reactivity	Low	Low

(a) at 25 °C, (b) viscosity of water at 25 °C is 0.890 mPa-s

3.2 Sample Introduction Technique

The calibration curves of lead with different introduction technique are plotted in Figure 3.

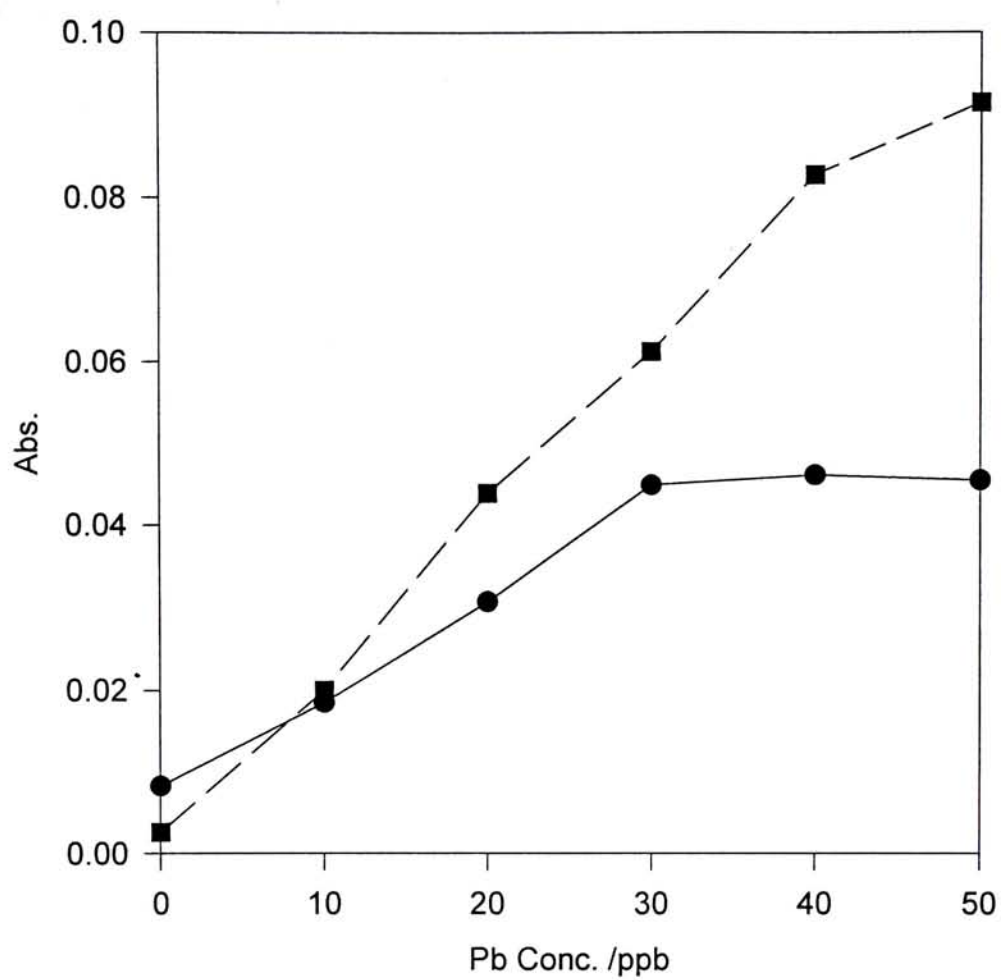


Figure 3. Variation of absorbance against lead concentration.
—●— Direct Introduction
—■— Platform in tube

The lead calibration curve bent downwards at high concentration by direct introduction technique whereas it could keep linear by platform in tube technique. It indicated that using platform in tube technique would give a much better result on the determination of lead by GFAAS.

With the sample directly deposited on the tube wall, the sample was evaporated and ashed on the tube wall. When the tube temperature was raised rapidly, the sample followed this temperature rise. As a consequence, atomization occurred in an environment in which the temperature was changed so rapidly and hence less reproducible results were obtained.

With the presence of graphite platform inside the tube, the sample was deposited on the small platform surface rather than on the inside wall of the tube. The platform was primarily heated by radiation from the tube wall, so that a time lag existed between heating of the tube and the platform. When the graphite tube was heated rapidly in the atomization step, the temperature of the platform followed this temperature rise slowly. The platform reached the atomization temperature when the tube wall and the gas had already reached equilibrium. The temperature of the gas was higher than that of the platform. The atoms of the analyte were thus volatilized in a gas with a higher temperature at equilibrium, so that chemical interferences were diminished. Therefore, platform in tube technique was better than direct introduction technique and hence chosen for subsequent studies.

3.3 Recovery Study of lead in SRM in 1-Decanol

The amount of lead in SRM under (a) 1-decanol and (b) acid digestion is known in Table 4.

Table 4. Amount of lead in SRM under (a) 1-decanol (b) acid digestion.

<i>Trial</i>	<i>Amount of lead in 1-decanol (ppb)</i>	<i>Amount of lead by acid digestion (ppb)</i>
1	30.44	23.24
2	23.30	24.91
3	19.59	19.64
4	25.70	22.72
<i>Results</i>	Mean = 24.76 ppb RSD = 18.3 % (n = 4) Certified amount = 53 ppb Recovery = 46 %	Mean = 22.62 ppb RSD = 9.7 % (n = 4) Certified amount = 27.8 ppb Recovery = 81 %

The recovery of lead in SRM under 1-decanol was 46 %, which was abnormally low compared with 81 % recovery by the acid digestion method.

The low recovery of lead in 1-decanol could be explained by the following factors:

3.3.1 Drying stage of the temperature program for analysis

The inclusion of the drying stage was to dry the sample so as to prevent abrupt boiling at the ashing and atomizing stages. Therefore, the temperature at this stage should be high enough for the complete removal of the solvent. Also, it should have enough time for the drying of the sample or the sample splashed due to abrupt evaporation. Since 1-decanol had a much higher boiling point than water, the upper limit of the drying stage was increased from 140 °C to 200 °C so as to completely remove the organic solvent away.

3.3.2 Effect of 1-decanol on the absorbance signal of the analyte

As the injection volume of 1-decanol increased, the recovery was decreased. This could be best visualized by the addition of 1-decanol on aqueous samples.

For each 20 μL aqueous sample of SRM analyzed, 0 - 20 μL 1-decanol was added to it. The volume of 1-decanol added was monitored as the change in the recovery. The results are summarized in Table 5.

Table 5. The change in recovery with the volume of 1-decanol added.

<i>Volume of 1-decanol added for 20 μL aqueous sample (μL)</i>	<i>Recovery of lead in aqueous sample (%)</i>	<i>Remarks</i>
0	92	
5	63	
15	61	ABS < REF
20	N/A (Over Background)	ABS < REF

From the results, it showed that increasing the volume of 1-decanol added decreased the recovery of aqueous samples. The presence of organic solvent would suppress the absorbance signal of the analyte and hence the recovery.

Besides, as the volume of 1-decanol increased, the absorbance signal of the analyte was less than the reference signal, which was abnormal. This phenomenon could be explained by the design of temperature program and the injection volume.

The 1-decanol was an organic solvent with a high boiling point. Therefore, large volume of it could not be completely removed during the drying step of the temperature program in GFAAS. It would become a background absorption and hence affect the results.

3.3.3 Sample injection volume

The maximum allowable injection volume of the graphite tube used in this GFAAS was 50 μL . However, half or less of the maximum volume should be injected to prevent interference and background absorption by minimizing the absolute quantity of coexisting substances.

Since the sample was deposited on the small platform surface rather than the tube wall, the sample injection volume should be small to prevent the spreading of sample from the platform surface. Therefore, the sample injection volume was maintained at 10 μL in the subsequent studies.

3.3.4 Design of temperature program for analysis

In order to effectively remove the solvent, the temperature of the drying stage was set from 80 - 280 $^{\circ}\text{C}$ for 100 seconds to evaporate 1-decanol from the sample at a moderate heating rate.

At the ashing stage the sample was ashed to eliminate interference due to background absorption. The ashing temperature should not be too high or it would cause the loss of the object element. Since lead was a volatile element, the ashing temperature was maintained at 400 $^{\circ}\text{C}$ to prevent the evaporation of lead in this stage.

The analyte element was atomized during the atomizing step. The temperature for atomization depends on the element of interest and it was maintained at 2000 $^{\circ}\text{C}$ for lead since a high atomizing temperature accelerated the atomizing speed and shortened the retention time of atomic vapor in the graphite tube.

Table 6 summarizes the parameters employed in the analysis of lead by GFAAS in the subsequent studies.

Table 6. Parameters employed for the analysis of lead by GFAAS.

<i>Sample introduction technique</i>			Platform in tube	
<i>Sample injection volume</i>			10 μL	
<i>Temperature program</i>				
<i>Stage</i>	<i>Start (°C)</i>	<i>End (°C)</i>	<i>Ramp (s)</i>	<i>Hold (s)</i>
Drying	80	280	100	
Ashing	400	400	30	
Atomizing	2000	2000		10
Cleaning	2200	2200		4
Cooling				5

With the new parameters employed, the results of recovery of lead in SRM under 1-decanol are shown in Table 7.

Table 7. Amount of lead in SRM under 1-decanol (by new analytical parameters).

<i>Trial</i>	<i>Amount of lead in 1-decanol (ppb)</i>
1	31.69
2	28.63
3	28.74
<i>Results</i>	Mean = 29.69 ppb RSD = 5.8 % (n = 3) Certified amount = 53 ppb Recovery = 56 %

The recovery of lead in SRM under 1-decanol using new analytical parameters was 56 %. Compared with previous analytical technique which gave 46 % recovery of lead in SRM, there was 10 % improvement.

3.4 Study of Suspension Behavior of Solvents

Laser light particle size analyzer used laser light with a wavelength of 750 nm to size particles with diameters from 0.4 μm to 2000 μm by light diffraction.⁵² The laser's radiation passed through a spatial filter and projection lens to form a beam of light. The beam passed through the sample cell where particles suspended in liquid scattered the incident light in characteristic patterns which depended on their sizes.

The analyzer measured particle size distribution by measuring the pattern of light scattered by the constituent particles in the sample. This pattern of scattered light was called a diffraction pattern. Each particle's diffraction pattern was characteristic of its size. The pattern measured by the analyzer was the sum of the patterns scattered by each constituent particle in the sample. An important component for making this measurement in the analyzer was the Fourier lens. The lens focused any light striking any part of the lens at a given angle onto a single annular area on its plane of focus, the Fourier plane. The Fourier lens was sensitive only to the angle of the light rays incident on it and not to the position or velocity of the source of light. The result was that the Fourier lens formed an image of the entire diffraction pattern of each particle, the image being centered at a fixed spot on the Fourier plane. The individual diffraction patterns from the many moving particles in the sample cell were therefore superimposed, creating a single composite diffraction pattern that reflected the contributions from all the particles in the sample cell. This

composite diffraction pattern can be accurately sensed by detectors placed on the Fourier plane. Over the course of a measurement, a running average was computed on the flux pattern at every instant. When the duration of the measurement was long enough that the flux pattern accurately represented the contributions from all sample particles, an analysis of the resulting pattern would yield the true particle size distribution of the sample.

A solvent having high viscosity did not necessarily provide a stable suspension of the air particulates. Therefore, the suspension property of the chosen solvents was studied.

The settling behavior of the SRM in these solvents was observed. The distribution and the change in mean particle size of particulate matter in the solvent was monitored by a laser light particle size analyzer. The result is summarized in Table 8.

Table 8. Comparison of the suspension behavior of ethylene glycol and 1-decanol.

<i>Time (mins.)</i>	<i>in ethylene glycol (μm)</i>	<i>in 1-decanol (μm)</i>
0	4.9	5.1
5	4.8	3.5

The distribution of particle size of Urban Air Particulate under these solvents is known in Figure 4 and 5.

At the beginning, the mean particle size of SRM under the 2 solvents was about 5 μm , which was a typical particle size of RSP.

However, the settling of air particulates was more severe in 1-decanol than in ethylene glycol after 5 minutes. The mean particle size of particulate matter in 1-

decanol seriously dropped from 5.1 μm to 3.5 μm , indicating that the larger and heavier particles settled to the bottom during this period, leaving smaller and lighter particulate matter in the solvent media. Therefore, the mean particle size of particulate matter in 1-decanol decreased.

There was no sufficient change in mean particle size of particulate matter in ethylene glycol during the 5-minute period, indicating that ethylene glycol suspended and hence distributed the particulate matter well in the solvent media.

In view of this result, ethylene glycol was chosen as the suspending media of the particulate matter for subsequent analysis.

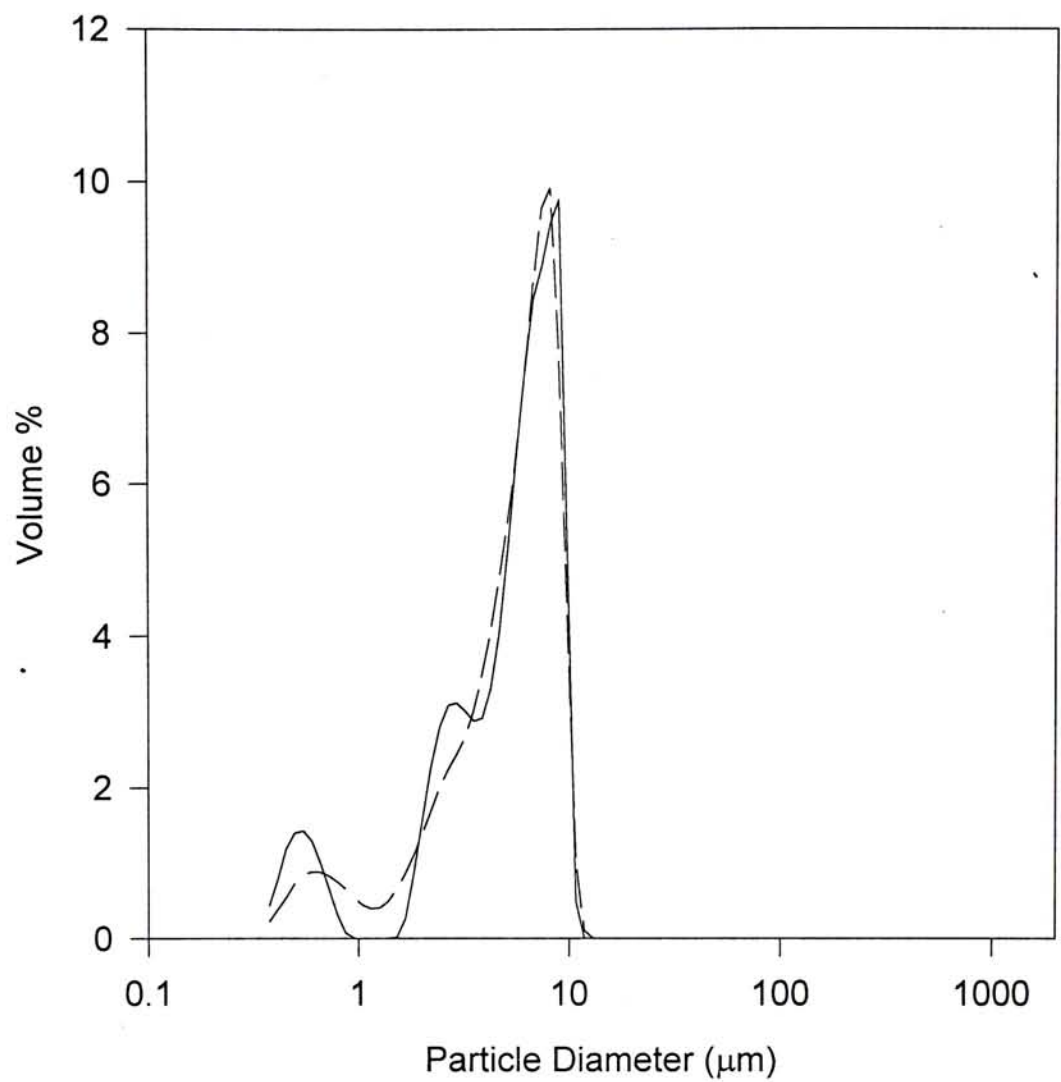


Figure 4. Distribution of the particle size of urban particulate matter in ethylene glycol.

— $t = 0$
- - $t = 5$ minutes

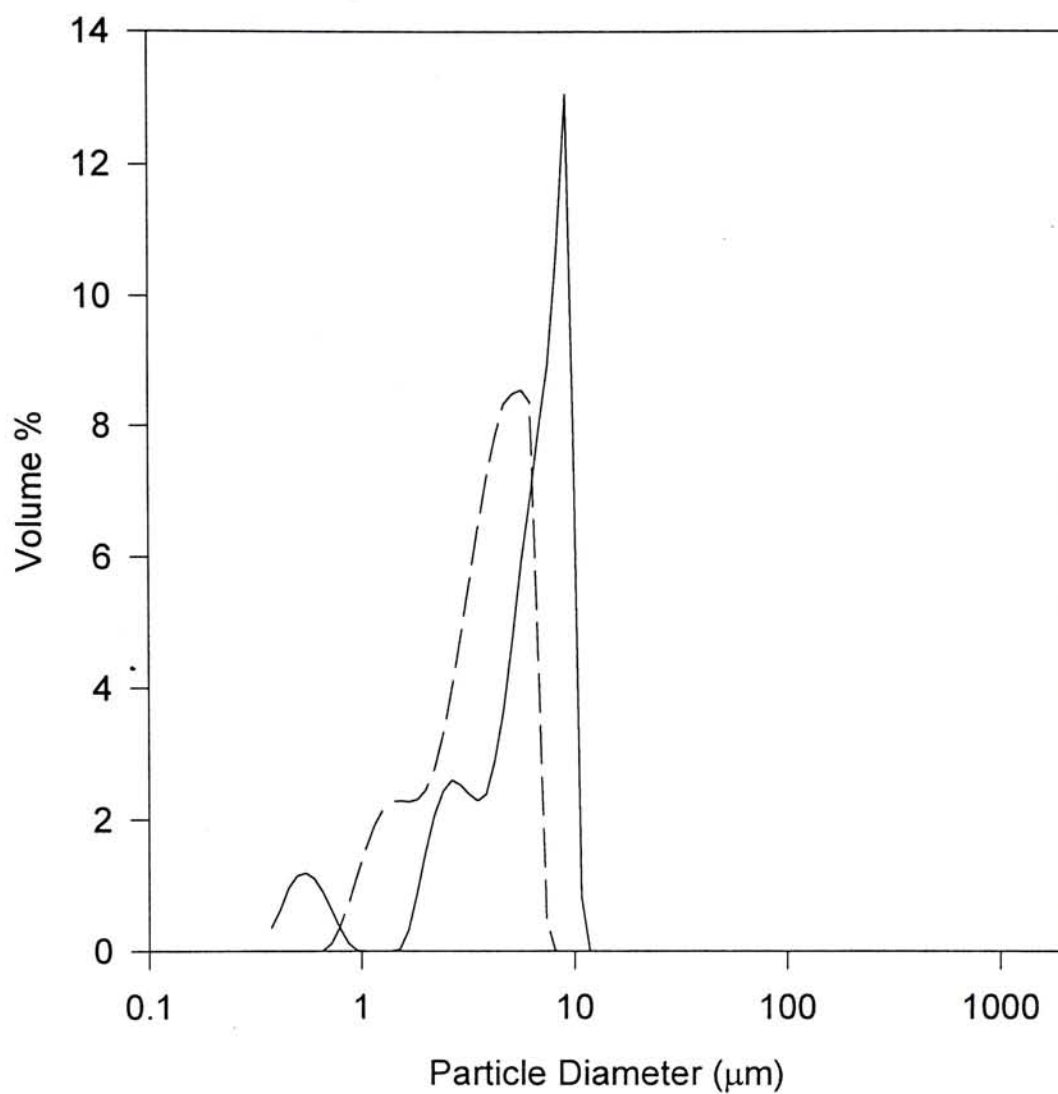


Figure 5. Distribution of the particle size of urban particulate matter in 1-decanol.

— $t = 0$
- - $t = 5$ minutes

3.5 Recovery Study of lead in SRM in Ethylene Glycol

The results showing the recovery of lead under ethylene glycol are given in Table 9.

Table 9. Amount of lead in SRM under ethylene glycol.	
<i>Trial</i>	<i>Amount of lead in ethylene glycol (ppb)</i>
1	35.71
2	26.00
3	29.14
4	37.33
<i>Results</i>	Mean = 32.00 ppb RSD = 16.7 % (n = 4) Certified amount = 54 ppb Recovery = 60 %

The recovery of lead under ethylene glycol was 60 %. It was slightly better than under 1-decanol but still far from satisfactory when compared with the recovery based on acid digestion. The low recoveries of the two solvents were due to the matrix effect as the amount of lead in the chosen solvents was compared with the aqueous calibration curve. Therefore, standard addition method was used to compensate the matrix interference in the subsequent analysis.

3.6 Evaluation of the Developed Method

3.6.1 Determination of lead in SRM

Table 10. The absorbance data of Pb in sample by GFAAS.

	<i>Trial 1</i>	<i>Trial 2</i>	<i>Trial 3</i>
<i>Volume of Pb standard added (μL)</i>	<i>Mean absorbance (n = 3)</i>	<i>Mean absorbance (n = 3)</i>	<i>Mean absorbance (n = 3)</i>
0	0.1959	0.2148	0.2157
20	0.2419	0.2621	0.2651
40	0.3073	0.3055	0.3072
60	0.3404	0.3369	0.3479

Table 10 summarizes the absorbance data of each trial. The amount of lead in each trial was calculated by standard addition method and then compared with the certified value in SRM. The results are shown in Table 11.

Table 11. Comparison between measured and certified concentration of Pb in SRM.

<i>Trial</i>	<i>Certified Conc. of Pb in SRM (ppb)</i>	<i>Measured Conc. of Pb in SRM (ppb)</i>	<i>Recovery (%)</i>
1	262	393	150
2	363	546	150
3	363	495	137

The conditions of standard addition method and the Zeeman correction effect incorporated in GFAAS were accounted for the abnormally high values on recovery.

The use of standard addition method relied on the assumptions that (1) a linear relationship existed between the absorbance y and the concentration of the analyte x and (2) the sensitivity was not changed by the additions.

Therefore standard addition method could only be applied under the limited linear range of the calibration curve. Besides, the concentration of the analyte should not be high or the sensitivity would be changed during the additions.

Although the Zeeman correction effect could effectively correct for the background absorption from the analyte, it had some shortcomings.

The Zeeman effect split the absorption line of the analyte into π - (central line) and σ - (sidebands) components. As the concentration of the analyte increased, the sidebands broadened and began to absorb more and more of the perpendicular component of the source radiation. The analyte absorbance was considered as background and subtracted, causing the working curve to bend downwards. Therefore, the usable working range decreased and hence the concentration above this range would have lower absorbance than expected.

Many elements did not undergo normal Zeeman splitting but instead yielded complex anomalous patterns. The pattern with three split lines like Cd 228.8 nm is called a normal Zeeman pattern. The pattern with split π -component lines like Cu 324.8 nm is called an anomalous Zeeman pattern. Since splitting was usually not completed, there was some atomic absorption included in the background measurement and hence the sensitivity was reduced.⁴⁶ Furthermore, due to transmission losses in polarizer components and the use of only a fraction of the field-free source intensity for each measurement, the source intensity was reduced.

Since the Zeeman effect significantly decreased the usable working range and sensitivity of the calibration curve, the calculation on the concentration of lead in SRM based on standard addition method showed a great discrepancy.

To apply the developed method in measuring lead content in air particulates that have varying concentration in different regions, the non-linear standard addition method was applied.

3.6.2 Application of non-linear standard addition method

It had been reported in the literature⁴⁸⁻⁵¹ that the non-linear standard addition method could successfully determine the metal content in the sample. However, this method usually involved tedious calculations. In order to simplify the calculation, the relationship between the absorbance and the concentration of the analyte could be determined by using a non-linear regression program which was usually found in a spreadsheet software, such as Excel[®].

By fitting the absorbance data in Table 10 using the non-linear regression program, the relation between the absorbance (y) and the volume of standard added (x) could be determined (Table 12).

Table 12. Curve fitting results using non-linear regression program.

Trial	Non-linear regression equation	Regression coefficient, R^2
1	$y = -8 \times 10^{-6} x^2 + 0.003x + 0.1933$	0.9894
2	$y = -1 \times 10^{-5} x^2 + 0.0026x + 0.2144$	0.9996
3	$y = -5 \times 10^{-6} x^2 + 0.0025x + 0.216$	0.9998

Hence the concentration of lead in sample was known and it is compared with the certified concentration in SRM 1648 (Table 13).

Table 13. Comparison between measured and certified concentration of Pb in SRM with non-linear standard addition based on ethylene glycol.

<i>Trial</i>	<i>Certified Conc. of Pb in SRM (ppb)</i>	<i>Measured Conc. of Pb in SRM (ppb)</i>	<i>Recovery (%)</i>
1	262	280	107
2	363	329	91
3	363	375	103

With the non-linear standard addition method, the recovery was significantly improved.

3.6.3 Precision and accuracy of the developed method

The precision that was expressed as percentage relative standard deviation in the absorbance of 3 replicate measurements of the sample was $\pm 4\%$. The accuracy that was expressed as percentage recovery between the certified and measured concentration of lead in SRM was between 91 - 107 %.

3.7 Recovery Study with the Acid Digestion Method

By the acid digestion method the recovery on the determination of lead in SRM was 81 %. Less than 100 % recovery was explained by the sample loss during the digestion and dilution processes.

3.8 Analysis of Real Samples by the Developed Method

3.8.1 Principles of TEOM[®] on mass measurement

Tapered-element oscillating balance (TEOM) was a balance that could precisely monitor particulates as they were sampled - in real time, on site, on line. It was a hollow, tapered element with the wide end fixed and the narrow end holding a disc-like filter cartridge. For mass measurement, the resonant frequency of the hollow, tapered element in a clamped-free mode was used. The particulates were collected on the filter from the gas drawn through it, and the filtered gas proceeded through the hollow element. Since the mass of the filter increased as the deposited mass increased, the vibrational frequency of the tapered element decreased according to the relation:

$$m = k_0 (f_1^{-2} - f_0^{-2})$$

where m	=	mass deposited on the filter
k_0	=	calibration constant
f_0	=	frequency before addition of deposited mass
f_1	=	frequency after mass deposition

With the relation between the mass and the vibrational frequency, the mass of particulates deposited was determined.

3.8.2 Selection of filter media for air sampling

3 types of filter media, cellulose acetate, quartz fiber and Teflon filter, were chosen in this research. Among the three types of filters under studied, Teflon filter offered many advantages on particulate dislodging over the others.

Teflon filters were inert to chemical transformations, extremely low moisture sensitivity and background concentrations.¹¹ Besides, the particulates collected on

the filter surface was easily dislodged with ultrasonic agitation whereas it was difficult to remove from the cellulose acetate filter due to the buildup of electrostatic charge on the filter surface. Quartz fiber filter was friable so some fibers would also be removed from the filter surface on ultrasonic agitation. Moreover, the particulates collected were distributed throughout the depth of quartz fiber filter so it was difficult to remove the particulates from it.

However, Teflon filter was not free from defects. The ring that was used to support the Teflon filter would introduce sample contamination during particulate dislodging. The temperature range of supported Teflon filter was about 150 °C, which was much lower than quartz fiber filter that could be stable up to 800 °C.¹¹ Moreover, Teflon filter was much more expensive than cellulose acetate filter.

Since Teflon filter showed promising results on particle dislodging, it was chosen for collection of air particulates.

3.8.3 Study of dislodging efficiency of air particulates from Teflon filter

The transfer of air particulates from Teflon filter to ethylene glycol was an essential step in sample treatment. The amount of air particulates removed would affect the accuracy of subsequent analysis.

The amount of air particulates removed by ultrasonic agitation was 0.50 mg and the mass of RSP collected at Cape D'Aguilar during the sampling period was 0.59 mg. Hence, the dislodging efficiency was 84 %.

3.8.4 Comparison with the acid digestion method

Table 14. The absorbance data of lead in real sample.

<i>Volume of Pb standard added (μL)</i>	<i>Mean absorbance (n = 3)</i>
0	0.0333
20	0.0899
40	0.1390

Table 14 summarizes the absorbance data of real sample by developed method. The relation between the absorbance and the volume of standard added is determined by non-linear regression program (Table 15).

Table 15. Curve fitting results using non-linear regression model. (real sample)

Sample	Non-linear regression equation	Regression coefficient, R ²
1	$y = -9 \times 10^{-6} x^2 + 0.003x + 0.0333$	1

The amount of lead collected on the filter was determined and the result was compared with that obtained by acid digestion method. The results were shown in Table 16. From the results, it showed a good agreement between the two methods.

Table 16. Comparison between the developed and acid digestion method on the analysis of lead in real sample.

	<i>Developed Method</i>	<i>Acid Digestion Method</i>
Amount of lead (ng/m ³)	27 ± 3	22 ± 3

4. Conclusion

Acid digestion is a standard treatment method for metals in air particulates. However, it suffers from potential contamination and loss of volatile element during the time-consuming process.

Suspension of air particulates in ethylene glycol allows the direct determination of lead with graphite furnace atomic absorption spectrometry. Ethylene glycol was a good solvent for suspending the particulate matter. With non-linear standard addition technique, the developed method can determine the metals in wide concentration range. Unlike the acid digestion method, this method is accurate, fast and virtually free of contamination.

5. References

1. Environmental Protection Department *Environment Hong Kong 1996*, Hong Kong, 1996; p. 19.
2. Planning, Environment and Lands Branch, Hong Kong Government *White Paper The Third Review*, Hong Kong, 1996; Chapter 2.
3. Lam, S. H.; Gervat, G. P.; Laboratory Management Section, Environmental Protection Department *Air Quality in Hong Kong 1994*, Hong Kong, 1996; Chapter 4 - 6.
4. Pun, W. M.; Gervat, G. P., Environmental Protection Department *Air Quality in Hong Kong 1989*, Hong Kong, 1993; Table 19.
5. Pun, W. M., Environmental Protection Department *Air Quality in Hong Kong 1990*, Hong Kong, 1993; Table 20.
6. Pun, W. M., Environmental Protection Department *Air Quality in Hong Kong 1991*, Hong Kong, 1993; Table 19.
7. Gervat, G. P., Environmental Protection Department *Air Quality in Hong Kong 1992*, Hong Kong, 1994; Table B10(b).
8. Gervat, G. P., Environmental Protection Department *Air Quality in Hong Kong 1993*, Hong Kong, 1995; Table 12.
9. Lam, S. H.; Gervat, G. P.; Laboratory Management Section, Environmental Protection Department *Air Quality in Hong Kong 1994*, Hong Kong, 1996; Table 7(a).
10. Office of Air Quality Planning and Standards, *US Environmental Protection Agency Health Effects Notebook for Hazardous Air Pollutants*, 1994. (URL: <http://www.epa.gov/oar/oaqps/airtox/hapindex.html>)

11. Lee, K. W; Ramamurthi, M. In *Aerosol Measurement: Principles, Techniques, and Applications*, Willeke, K.; Baron, P. A., Eds.; Van Nostrand Reinhold: New York, 1993; Chapter 10.
12. Lippmann, M. In *Methods of Air Sampling and Analysis*, Lodge, J. P. JR., Eds.; Lewis Publishers: Chelsea, 1988; Part I.
13. Wight, G. D. *Fundamentals of Air Sampling*; Lewis Publishers: Boca Raton, 1994; Chapter 7.
14. Vandecasteele, C; Block, C. B. *Modern Methods for Trace Element Determination*; Wiley: New York, 1993.
15. Bendicho, C.; De Loos Vollebregt, M. T. C. *Journal of Analytical Atomic Spectrometry*, **1991**, 6, 353-374.
16. Milacic, R.; Dolinsek, F. *International Journal of Environmental Analytical Chemistry*, **1994**, 57, 329-337.
17. Carneiro, M. C.; Campos, R. C.; Curtius, A. J., R. *Talanta*, **1993**, 12, 1815-1822.
18. Cabrera, C.; Lorenzo, M. L.; Lopez, M. C. *J. AOAC Int.*, **1995**, 78, 1061-1067.
19. Dalen, G.; de Galan, L. *Spectrochimica Acta, Part B*, **1994**, 49B, 1689-1693.
20. Vinas, P.; Campillo, N.; Lopez Garcia, I.; Hernandez Cordoba, M. *Food Chemistry*, **1994**, 50, 317-321.
21. Vinas, P.; Campillo, N.; Lopez Garcia, I.; Hernandez Cordoba, M. *Atomic Spectroscopy*, **1995**, 16, 86-89.
22. Vinas, P.; Campillo, N.; Lopez Garcia, I.; Hernandez Cordoba, M. *Talanta*, **1995**, 42, 527-533.
23. Dobrowolski, R.; Mierzwa, J. *Fresenius' Journal of Analytical Chemistry*, **1993**, 346, 1058-1061.

24. Kukier, U.; Sumner, M. E.; Miller, W. P. *Commun. Soil Sci. Plant Anal.*, **1994**, *25*, 1149-1159.
25. Lopez-Garcia, I.; Sanchez-Merlos, M.; Hernandez-Cordoba, M. *Anal. Chim. Acta*, **1996**, *328*, 19-25.
26. Deng, S. L.; Li, X. F.; Zhou, P. *Guangpuxue Yu Guangpu Fenxi*, **1996**, *16*, 106-110.
27. Dobrowolski, R. *Spectrochimica Acta*, Part B, **1996**, *51B*, 221-227.
28. Bermejo-Barrera, P.; Barciela-Alonso, M. C.; Moreda-Pineiro, J.; Gonzalez-Sixto, C.; Bermejo-Barrera, A. *Spectrochimica Acta, Part B*, **1996**, *51B*, 1235-1244.
29. Bermejo-Barrera, P.; Moreda-Pineiro, J.; Moreda-Pineiro, A.; Bermejo-Barrera, A. *Anal. Chim. Acta, Part B*, **1994**, *296*, 181-193.
30. Bermejo-Barrera, P.; Barciela-Alonso, C.; Aboal-Somoza, M.; Bermejo-Barrera, A. *Journal of Analytical Atomic Spectrometry*, **1994**, *9*, 469-475.
31. Spellmaecker, M.; Ouddane, B.; Fisher, J. C.; Wartel, M.; Hoenig, M. *Analisis*, **1996**, *24*, 76-78.
32. Morita, Y.; Isozaki, A. *Bunseki Kagaku*, **1995**, *44*, 703-707.
33. Cabrera, C.; Lorenzo, M. L.; Lopez, M. C. *J. Agric. Food Chem.*, **1995**, *43*, 1605-1609.
34. Arruda, M. A. Z.; Gallego, M.; Valcarcel, M. *Journal of Analytical Atomic Spectrometry*, **1995**, *10*, 55-59.
35. Vinas, P.; Campillo, N.; Lopez Garcia, I.; Hernandez Cordoba, M. *Fresenius' Journal of Analytical Chemistry*, **1995**, *351*, 695-696.
36. Vinas, P.; Campillo, N.; Lopez Garcia, I.; Hernandez Cordoba, M. *Analyst*, **1994**, *119*, 1119-1123.

37. Shiowatana, J.; Siripinyanond, A. *Atomic Spectroscopy*, **1996**, *17*, 122-127.
38. Bendicho, C.; Sancho, A. *Atomic Spectroscopy*, **1993**, *14*, 187-190.
39. Vinas, P.; Campillo, N.; Lopez Garcia, I.; Hernandez Cordoba, M. *Fresenius' Journal of Analytical Chemistry*, **1994**, *349*, 306-310.
40. Vinas, P.; Campillo, N.; Lopez Garcia, I.; Hernandez Cordoba, M. *J. Agric. Food Chem.*, **1993** *41*, 2024-2027.
41. Lopez-Garcia, I.; Vinas, P.; Campillo, N.; Hernandez-Cordoba, M. *J. Agric. Food Chem.*, **1996** *44*, 836-841.
42. Bermejo-Barrera, P.; Lorenzo Alonso, M. J.; Aboal-Somoza, M.; Bermejo Barrera, A. *Mikrochim. Acta*, **1994**, *117*, 49-64.
43. Bermejo-Barrera, P.; Moreda-Pineiro, A.; Romero-Barbeito, T.; Moreda-Pineiro, J.; Bermejo-Barrera, A. *Talanta*, **1996**, *43*, 1099-1107.
44. Pita Calvo, C.; Bermejo Barrera, P.; Bermejo Barrera, A. *Anal. Chim. Acta*, **1995**, *310*, 189-198.
45. Skoog, D. A.; Leary, J. J. *Principles of Instrumental Analysis*; Saunders College Publishing: Fort Worth, 1992; Chapter 10.
46. Hitachi Ltd. In *Graphite Atomization Analysis Guide for Polarized Zeeman Atomic Absorption Spectrophotometry*; Hitachi Ltd.: Japan 1992; Application Note.
47. Chakrabarti, C. L.; Xiuren, H.; Shaole, W.; Schroeder, W. H. *Spectrochimica Acta*, **1987**, *42B*, 1227-1233.
48. Favretto, L.; Marletta, G. P.; Favretto, L. G. *Atomic Spectroscopy*, **1984**, *5*, 51-54.
49. Liu, Y.; Li, S. *Fenxi Huaxue*, **1986**, *14*, 110-116.
50. Mueller, M. A.; Oelschlaeger, H. *Fresenius' Journal of Analytical Chemistry*, **1981**, *307*, 109-114.

51. Andersson, M.; Olin, A. *Talanta*, **1991**, 38, 385-390.
52. Coulter Corporation In *Coulter LS series Product Manual*.; Coulter Corporation: USA 1994; Manual.
53. Chakrabarti, C. L.; Marchand, B.; Vandernoot, V; Walker, J.; Schroeder, W. H. *Spectrochimica Acta*, **1996**, 51B, 155-163.

6. Appendix

Preliminary Study on Graphite Platforms Filtration and Atomization

Introduction

Electrographite has a porous structure with the presence of micropores inside it.⁴⁷ Therefore, the graphite can be fabricated into a thin platform so that it can act as a filter to collect the air particulates from the air with the incorporation of specially designed sampler. Besides, the graphite platform loaded with air particulates can be directly introduced into the graphite tube of GFAAS for analysis.

Some Examples of Graphite Platforms Atomization Systems

*L'vov platform technique*¹⁵

The platform made of pyrolytic graphite is inserted into the center of a graphite tube. The sample is deposited on the platform. The platform is mainly heated by radiation from the hot tube wall.

*Graphite probe atomizer*¹⁵

A probe of graphite is inserted into a graphite tube that is preheated to atomization temperature. As the probe is primarily heated by radiation transfer from the hot tube, atomization of the analyte takes place at a constant temperature of the gas phase.

Experimental

A sampling device was developed with slight modification from Chakrabarti's design.^{47, 53} Figure A1 showed the schematic diagram of the sampling device. It consisted of two blocks (upper and lower) made of Teflon where a porous

graphite platform ($3 \times 8 \times 0.5$ mm) was inserted inside the rectangular depression of the lower block of the sampling device.

A circular depression of 0.2 - 0.3 mm was made at the center of the graphite platform to enhance the filtration of air particulates. The graphite platform was cleaned, with the incorporation of the graphite tube, by heating at 2500 °C prior to use.

Stainless steel tubings (diameter = 3.2 mm) were connected to the upper and lower blocks of the sampling device. The sampling device was connected to a rotary vacuum pump by the stainless steel tubing at the lower block.

A graphite platform with porosity 24 % was inserted inside the depression of the sampling device. Air was drawn from the inlet of the stainless steel tubing at the upper block and air particulates was deposited on the graphite platform. After 30 minutes, the platform with air particulates collected was removed from the sampling device and put inside the graphite tube for the subsequent analysis by GFAAS.

Graphite platform filtration

The flow rate of the sampling device was about 100 mL/min at the beginning. As the filtration proceeded, the flow rate was decreased significantly. The reason for the drastic reduction in the flow rate was due to the blocking of the pores of the porous graphite by air particulates as the filtration proceeds. In order to increase the porosity of the porous graphite, annealing the graphite in an electric furnace at controlled temperatures (500 - 800 °C) was required.

However, annealing may result in enlarging the pore to a diameter that may allow air particulates of smaller size to pass through the graphite pores and not captured by the graphite filter, giving an erroneous value of the air particulates.

Thermal treatment of graphite platforms (annealing)

The graphite platform with porosity of 24 % was put in an oven of 800 °C for 1 hour. The platform was then inserted into the sampler for collecting the air particulates. It was found that the graphite platform showed greater flow rate after thermal treatment. It could be explained by the increase in the porosity of the graphite platform. This procedure deserved further investigation in order to find an optimum condition for annealing.

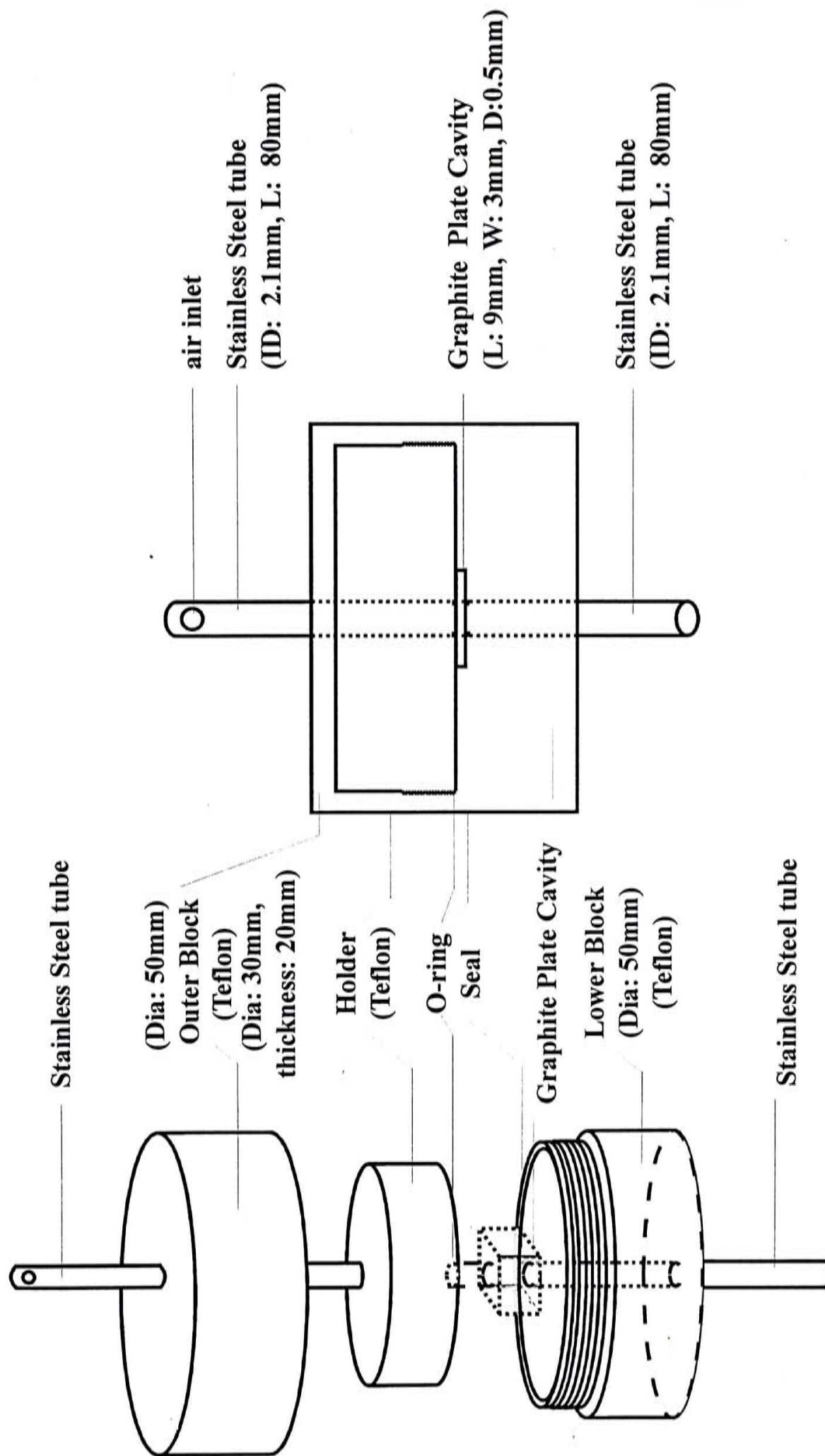
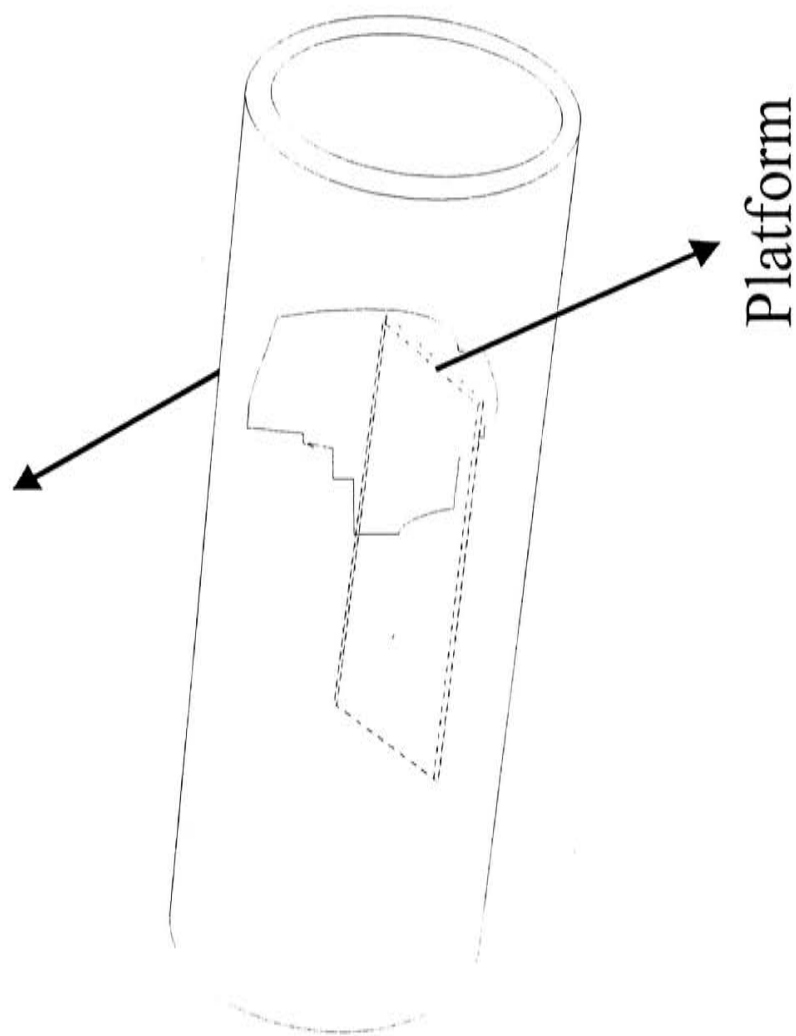


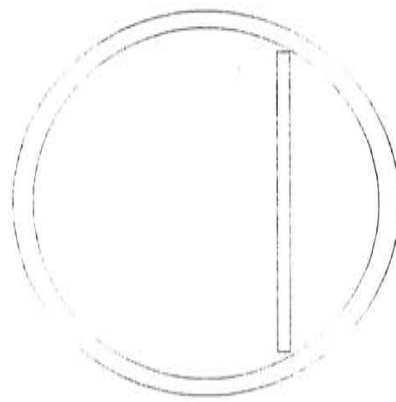
Figure A1. Schematic Diagram of Sampling Device.

Graphite Tube



Platform

(A) exposed view



(B) end view

Figure A2. Graphite tube with platform inside (A) exposed view (B) end view.

Table A1. Certified values of constituent elements in SRM 1648

<i>Major constituents</i>	<i>Content (Wt. Percent)</i>
Aluminum	3.42 ± 0.11
Iron	3.91 ± 0.10
Potassium	1.05 ± 0.01
<i>Minor constituents</i>	<i>Content (Wt. Percent)</i>
Lead	0.655 ± 0.008
Sodium	0.425 ± 0.002
Zinc	0.476 ± 0.014
<i>Trace constituents</i>	<i>Content ($\mu\text{g/g}$)</i>
Arsenic	115 ± 10
Cadmium	75 ± 7
Chromium	403 ± 12
Copper	609 ± 27
Nickel	82 ± 3
Selenium	27 ± 1
Uranium	5.5 ± 0.1
Vanadium	140 ± 3



CUHK Libraries



003589547